Identification of a new root rot-causing pathogen in Polygonatum cyrtonema Hua and screening of phytochemicals for its control

Guoyu Wei
Feng Wang
Wei Zhao
Huayang Xu
Guangming Wang
Hualei Wang
Anlong Hu (alhu@gzu.edu.cn)

Research Article

Keywords: Polygonatum cyrtonema Hua, root rot, Fusarium commune, biological characteristics, phytochemicals

Posted Date: July 18th, 2023

DOI: https://doi.org/10.21203/rs.3.rs-3130462/v1

Identification of a new root rot-causing pathogen in *Polygonatum cyrtonema* Hua and screening of phytochemicals for its control

Guoyu Wei[1], Feng Wang[2], Wei Zhao[1], Huayang Xu[1], Guangming Wang[3], Hualei Wang[1], Anlong Hu[1,*]

[1] College of Agriculture, Guizhou University, Guizhou 550025, Guiyang, China
[2] Zaozhuang Vocational College,Shandong 277000, Zaozhuang, China
[3] Guizhou Province Qiansheng Taijiang Poverty Alleviation Industry Development Co., Ltd. Guizhou 556300, Taijiang, China

Abstract: *Polygonatum cyrtonema* Hua is a perennial herb belonging to the Liliaceae family, with significant medicinal and dietary value. However, root rot， a server disease, has led to a decline in yield and quality of this species. In this study, a fungus was isolated from symptomatic samples of root rot and identified as *Fusarium commune* through molecular and morphological analyses. After re-isolation, the identification of *F. commune* as the causative agent of root rot was confirmed by fulfilling Koch's postulates in subsequent tests.. Biological characteristics indicated that the optimal growth conditions for *F. commune* were a temperature of 25℃, pH of 8, carbon source of soluble starch, nitrogen source of peptone, and a photoperiod of 24 hours. In order to reduce the use of chemical fungicides and explore natural substances to control the disease, the sensitivity of *F. commune* to seven phytochemicals was studied. Four phytochemicals showed apparent inhibitory activity and honokiol displaying the highest antifungal activity, having a 50% of the maximal effect concentration (EC_{50}) of 8.2628 ± 0.27 mg/L. These findings provide a scientific basis for the control of root rot in *P. cyrtonema* Hua.

Keywords: *Polygonatum cyrtonema* Hua; root rot; *Fusarium commune;* biological characteristics; phytochemicals

1. Introduction

Polygonatum, a genus in the Liliaceae family commonly known as Solomon's seal, is primarily distributed in China, North Korea, Russia, India, Myanmar, and Mongolia (Sharma et al. 2021a). The genus has also been studied and cultivated in other countries, including the United States of America and Austria (Khan et al. 2010; Mottaghipisheh and Stuppner 2021). From the early to mid-1990s, the demand for Polygonatum remained stable at around 800 tons. By the end of 2019, the planting area of Polygonatum in China had expanded to approximately 4,000 ha, and the production had increased to about 18,000 tons due to economic development and increased demand for the plant's health benefits. The need for *Polygonatum* had increased to 3,000 tons for medicinal purposes, 12,000 tons for food processing applications, and 3,000 tons for *Polygonatum* extract production for processing and new product development.

Polygonatum cyrtonema Hua, commonly known as chicken head ginseng or tiger ginger, is a perennial herb that has been widely used in Chinese herbal medicine as valuable as *Polygonatum sibiricum* Red and *Polygonatum kingianum* Coll. Et Hemsl. Its rhizome is an excellent source of essential trace elements that provide multiple health benefits, such as lowering blood sugar, anti-tumor effects, improving immunity, and delayed aging (Liu et al. 2022; Wang et al. 2019; Hu et al. 2022; Luo et al. 2022; Chen et al. 2022a). Moreover, it holds high commercial value for new drugs development and health products creation. The supply of *P. cyrtonema* Hua has been predominantly based on wild resources for an extended period. However, the gradual

increase in market demand has led to large-scale artificial cultivation of this species. The condition of artificial cultivation have disruptedthe ecological balance of the original organisms of *P. cyrtonema* Hua leading to rampant pests and diseases. This situation adversely affects the growth and yield of *P. cyrtonema* Hua, posing a significant obstacle to the implementation of Good Agricultural Practice (GAP) for Chinese herbal medicine) and the development of modern medicine industry development. Additionally, it raises various safety hazards in the processing of Chinese herbal medicine products.

Root rot,caused by fungi, is a soil-borne disease that significantly restricts the yield and quality of *P. cyrtonema* Hua. In the early stages of this disease, the plants' aboveground parts do not show apparent symptoms. The leaves subsequently turn yellow from bottom to top, and the roots develop watery brown necrotic spots. As the disease progresses, the leaves slowly turn yellow from the outside to the inside, wilt from bottom to top, and ultimately causing the entire plant to wither and die. The underground rhizomes show expanding water stains and rot. When the disease is severe, only fibrous vascular bundles remain once the entire root has rotted. The affected parts appear brown or reddish-brown, with white mycelia visible on the surface of the rhizomes. Different fungal species, such as *Fusarium oxysporum*, *Fusarium solani*, and *Fusarium hostae*, are root rot pathogens that result in substantial economic losses (Ye et al., 2020; Özer et al., 2020).

F. commune, a member of the ascomycetes family, act as a causal pathogen for multiple diseases including butt rot in lotus (*Nelumbo nucifera*), rice (*Oryza*), alfalfa (*Medicago sativa*), and soybean (*Glycine max* (L.) Merr), stalk rot in tobacco (*Nicotiana tabacum*), and root and crown rot in maize (*Zea*). It alsocauses blight in potato (Deng et al. 2022; Husna 2020; Yang et al. 2022; Detranaltes et al. 2022; Mezzalama et al. 2021; Osawa et al. 2020). *F. commune* infestations in a field can lead to considerable reductions in yield (Audenaert et al. 2013). This pathogen produces mycotoxins that have poisonous effects on plants, animals, and humans (Arunachalam and Doohan 2013; Maresca 2013).

Temperature, light, pH, carbon, and nitrogen sources have a significant impact on the growth and pathogenicity of pathogenic fungi (Kaur et al. 2022; Telli et al. 2020; Kim et al. 2019; Tays et al. 2018). Therefore, it is crucial to study the biological characteristics of this pathogen，as well as the conditions that can trigger its occurrence and spread. Although chemical fungicides, such as benomyl, pyraclostrobin, and etridiazole, are commonly used to prevent and control root rot (Barbett and Sivasithamparam 1987; Wang et al. 2005; Lookabaugh et al. 2021), their repetitive use in high doses may lead to the development of pathogen resistance. Moreover, these fungicides have harmful environmental effects (Wu et al. 2019). Therefore, finding alternative disease control strategies is essential.. Previous research has shown phytochemicals, such as honokiol, magnolol, 2-allylphenol, eugenol, carvacrol, geraniol, and cinnamaldehyde, effectively combat plant pathogens (Qu et al., 2017; Yang et al., 2021; Zhou et al., 2019; Lima et al., 2017; Chen et al., 2019). Hence, exploring the use of phytochemicals as an alternative to chemical fungicides is a promising approach. Previous research has shown that phytochemicals, such as honokiol, magnolol, 2-allylphenol, eugenol, carvacrol, geraniol, and cinnamaldehyde, effectively combat plant pathogens (Qu et al., 2017; Yang et al., 2021; Zhou et al., 2019; Lima et al., 2017; Chen et al., 2019).

In July 2021, a typical case of root rot was observed in *P. cyrtonema* Hua in Tajiang County, Guizhou Province, China. The initial stages of the disease in the roots' belowground parts were characterized by water-stained brown necrotic spots that progressed to severe root rot, exhibiting a brown or reddish-brown color.. dentifying the underlying causes of *P. cyrtonema* Hua root rot and developing effective control methods are crucial for crop management and Chinese medicinal material cultivation. This study seeks to determine the pathogenic factors responsible for this disease, evaluate the pathogens' response to crucial environmental factors, and screen effective phytochemicals in vitro, providing a foundation for root rot control.

2. Materials and Methods

2.1. Pathogen isolation and purification

In 2021, a five-point survey method was employed to investigate sixteen fields of *P. cyrtonema* Hua in Taijiang County, Guizhou Province (26°66'91.6" N–108°31'81.4" E) . Each block (10 m^2) was assessed for the incidence rate of root rot, and samples exhibiting root rot symptoms were collected. Conventional tissue isolation methods were used, where in the symptomatic tissue samples were rinsed with sterile distilled water, followed by cutting them into approximately 1 cm × 1 cm slices using a sterile scalpel. The slices were then soaked into 75% alcohol for 30 s, disinfected for 1–2 min in 10% sodium hypochlorite, cleaned thrice with sterile water, drained using sterile paper, and dried in sterile Petri dishes. These dried symptomatic tissues were transferred to potato dextrose agar (PDA: 200.0 g potato, 20.0 g glucose, 17.0 g agar/L) plates on an ultra-clean at 25℃ inside a biochemical incubator (Ningbo Jiangnan Instrument Co., Ltd, Zhejiang, China). After 4 days of culture, the mycelia edge of typical single colonies were selected and purified repeatedly on PDA plate until pure colonies were obtained. These purified strains were cryopreserved with 30% glycerol and stored inside a refrigerator at -80℃ for further use.

2.2. Pathogenicity test of the isolated strain on *P. cyrtonema* Hua

The pathogenicity tested was conducted according to Koch's postulates (Zhang et al. 2021). The fungal isolates were cultivated on PDA at 25℃ for 7 d, while *F. commune* ZW0619 was cultured on carnation leaf-piece agar (CLA) medium to promote spore production (Choi et al. 2014). Spores were suspended in sterilized distilled water at a concentration of 10^6 conidia/mL, as determined using a cytometer (Solarbio Science and Technology Co., Ltd., Beijing, China). The pathogens were then inoculated into healthy *P. cyrtonema* Hua plants (Windham et al. 2018). The root and stem epidermis of healthy *P. cyrtonema* Hua were sprayed with 500 μL of 10^6 conidia/mL spore suspension or 500 μL sterile water as a control, and then transferred to a small bowl filled with sterilized soil. Three replicates were used for each isolate and the plants were incubated at 25℃, 85% relative humidity, and 12-h light/12-h dark for 14 days. The progression of the disease was recorded and the pathogens were re-isolated from the pathogenic sites for identification. The experiment was repeated thrice.

2.3. Morphological characterization

For morphological characterization, the isolated and purified pathogens were sampled using a 5-mm perforator at the edge of colonies. Fungus discs were then transferred to the center of a 9-cm PDA plate and on CLA for macroconidium production. The plates were inoculated at 25℃ for 7 d in a incubator for 7 days and the colony morphology and medium color were observed. The diameter of colony was measured as well. The shape of the hyphae and conidia of the representative isolates was observed under a binocular microscope (Leica DM500, Leica Microsystems (Shanghai) Trading Co., Ltd., Shanghai, China) equipped with a digital camera, and the size of conidia was measured. All experiment was repeated thrice.

2.4. Molecular identification of the pathogen

To identify the pathogen, targeted DNA sequence amplification and sequencing were performed. Fungal DNA was extracted from fresh aerial mycelia grown on PDA plates using a Fungal Genomic DNA Kit (Solarbio Science and Technology Co., Ltd., Beijing, China) according to the manufacturer's instructions. The amplification of translation elongation factor 1 alpha (*EF-1α*) RNA polymerase II encoding the second largest subunit (*RPB2*), and beta-tubulin (*TUB2*) (Table 1) was carried out. The PCR amplification procedure involved a final volume of 25 μL containing 12.5 μL of 2×Taq Master Mix (Sangong

Bioengineering Co., Ltd. (Shanghai)), 10 μM of each forward and reverse primer, 100 ng of DNA template, and ddH_2O. The cycling parameters followed the method described by Choi et al. (2010), including a denaturation step at 94℃ for 10 min followed by 35 cycles at 94℃ for 1 min, annealing at 60℃ (*TUB2* and *EF-1α*) or 64℃ (*RPB2*) for 1 min, and extension at 72℃ for 1 min, with a final extension step at 72℃ for 7 min and storage at 4℃. The PCR products were visualized on a 1.5% agarose gel prepared in 1× TAE using the BIO-RAD Gel Doc X.R.XR + Gel imaging system (BIO-RAD, Hercules, CA, USA), and the products were sent to Sangong Bioengineering Co., Ltd. (Shanghai) for sequencing. The measured gene sequences were spliced using ContigExpress, and the sequences were then uploaded to the GenBank database in NCBI (http://www.ncbi.nlm.nih.gov) for comparative analyses. A phylogenetic tree based on multigene sequences was constructed using the maximum likelihood (ML) method with 1000 bootstrap replications according to the method of Sharma and Kumar (2021b) using MEGA 7.0 (Kumar, 2018). Evolutionary distances were computed using the Kimura 2-parameter model (Kimura, 1980).

Table 1. PCR primers for *EF-1α*, *RPB2*, and *TUB2* gene amplification.

Target sequence	Primer	Primer sequence (5'–3')	Reference
TEF	EF1	ATGGGTAAGGAGGACAAGAC	O'Donnell et al. (1998)
	EF2	GGAGGTACCAGTGATCATGTT	
RPB2	RPB2-5f2	GCCGTCAACGACCCCTTCATT	O'Donnell et al. (2010)
	RPB2-7cr	GGGTGGAGTCGTACTTGAGCATGT	
TUB2	Bt2a	GGTAACCAAATCGGTGCTGCTTTC	Nosratabadi et al. (2018) Glass and Donaldson (1995)
	Bt2b	ACCCTCAGTGTAGTGACCCTTGGC	

2.5. Biobiological characteristics of ZW0619

The biological characteristics of the pathogen were investigated by assessing the effects of temperature, light, pH, and carbon and nitrogen sources on mycelial growth as described by Zhao et al. (2019) and Zambounis et al. (2020). To determine optimal growth conditions, the following experiments were conducted:.

(1) Effect of temperature on hyphae growth

The colony edges of ZW0619 after 5 days of incubation were taken useing a 5 mm hole punch, inoculated on new PDA plates, and incubated in light incubators at 10, 15, 20, 25, 28, 30, and 35℃, respectively. The mycelial growth was assessed by measuring the colony diameter after 5 days.

(2) Effect of light on hyphae growth

A 5-mm diameter hole punch was used to punch out the colonie discs to inoculate in the center of the PDA medium, and three treatments (24 h of full light, 24 h of full darkness, and 12-h light/12-h dark) were set to determine the optimal lighting conditions for mycelial growth. The strains were incubated in new PDA plates and incubated in a constant temperature incubator at 25℃ for 5 d.

(3) Effect of pH on hyphae growth

To assess the effect of pH on hyphal growth, the pathogen was cultured on PDA plates adjusted to pH 4, 5, 6, 7, 8, 9, and 10 using hydrochloric acid (1 mol·L^{-1}) or sodium hydroxide (1 mol·L^{-1}) 0.5 cm colonies are inoculated onto plates at different pHs and cultured in a constant temperature incubator at 25℃ for 5 d.

(4) Effects of carbon and nitrogen sources on the growth of the pathogen

Czapek medium (Czapek medium formula: 3 g sodium nitrate, 1 g dipotassium hydrogen phosphate, 0.5 g magnesium sulfate, 0.5 g potassium chloride, 0.01 g ferrous sulfate, 30 g sucrose, 15 g agar/L) was used as the base medium, and the sucrose was replaced with the same amount of glucose, lactose, soluble starch, fructose, glycerol or mannitol to make media with different carbon sources. A carbon-deficient medium was used as the control. Different nitrogen source media were prepared by replacing sodium nitrate in basal medium with equal amounts of ammonium sulfate, glycine, peptone, urea, beef paste, yeast paste or ammonium chloride, and a nitrogen-deficient medium was used as a control. A 0.5 cm of the colony was inoculated onto a medium containing different carbon sources and nitrogen sources,and the other steps were the same as the pH experiments on the growth of the pathogen.

The colony diameter for the temperature, light, pH, carbon and nitrogen sources tests was measured using the "ten" crossing method (Zhu et al. 2022; Chen et al. 2022). Three replicates were performed for each treatment.

2.6. In vitro toxicity tests

The in vitro toxicity of seven phytochemicals on the pathogen was determined using the mycelial growth rate method (Xing et al. 2017). All phytochemicals (Carvacrol, 2-Allylphenol, eugenol, honokiol, magnolol, cinnamaldehyde, geraniol) used in the study had purities of ≥95% and were provided by Aladdin Reagent Co., Ltd. (Shanghai, China). The phytochemicals were stored at 4℃ until use. Carvacrol, 2-Allylphenol, and eugenol were dissolved in ethanol, while honokiol and magnolol were dissolved in dimethyl sulfoxide, and cinnamaldehyde and geraniol were dissolved in acetone. The original solution of each agent was gradient-diluted based on the concentration range determined in the preliminary test.

Based on the concentration range determined in the preliminary test, the original solution of each agent was gradient-diluted. On an ultra-clean table, five effective concentrations of test agents were prepared with sterile water (Table 2). Five mL of each test phytochemical at various concentrations were added to 45 mL of PDA medium using a pipettor. The mixtures were sterilized, cooled to 55℃, and then mixed and shaken to prepare solid PDA plates with varying concentrations of phytochemicals. The water with the appropriate concentration of solvents was used as a control and three replicates for each treatment concentration were cooled and solidified. Holes were punched at the edge of the pathogen colony with a 5-mm hole punch, transferred to the center of the medium with a sterilized inoculation ring, sealed with a sealing film, and incubated at 25℃. After 5 d, the colony diameter for

different treatment concentrations was measured using the "+" crossing method, and the mean value and antifungal rate were calculated. The rate of inhibition of mycelial growth was determined using formula (1):

Growth inhibition rate (%) = 100 × (Dc − Dt) / (Dc − 0.5) (1)

Where Dc is the diameter of the colony on the control plate, 0.5 cm is the diameter of the inoculated mycelial disks, and Dt is the diameter of the colonies on plates with different concentrations of phytochemicals. The EC_{50} (concentration for 50% of the maximal effect) values of different phytochemicals were calculated using IBM SPSS analytics (SPSS Inc., Chicago, IL, USA) (Mo et al., 2021).

Table 2. Concentration gradients of the phytochemicals in the virulence assay experiments against ZW0619

Phytochemicals	Concentration Gradient (μg mL^{-1})				
	T1	T2	T3	T4	T5
2-Allylphenol	9.375	18.75	37.5	75	150
Eugenol	18.75	37.5	75	150	300
Carvacrol	9.375	18.75	37.5	75	150
Geraniol	18.75	37.5	75	150	300
Cinnamaldehyde	18.75	37.5	75	150	300
Honokiol	9.375	18.75	37.5	75	150
Magnolol	9.375	18.75	37.5	75	150

2.7. Data Analysis

The data were analyzed using Microsoft Excel 2021 (Microsoft Inc., Redmond, MA, USA), and plots were generated using OriginPro 2021 (OriginLab Corporation, Northampton, MA, USA). One-way analysis of variance (ANOVA) was conducted using DPS v16.0 (Ruifeng Information Technology Co., Ltd., Zhejiang, China), and Tukey's multi-range test was used to determine statistical significance at $P < 0.05$.

3. Results

3.1. Occurrence of root rot in P. cyrtonema Hua and field disease symptoms

In Guizhou Province, the root rot incidence in *P. cyrtonema* Hua was found to be more severe during the growth period (April to July), with an average incidence of 14%, which could increase up to 20% in severe cases. The rhizome was identified as the main site of disease occurrence. During the early stages of the disease, no obvious symptoms were observed on the leaves,however, water-stained brown necrotic spots were visible on the belowground roots accompanied by a fishlike smell. Under high humidity, white mildew could be observed on the surface of *P. cyrtonema* Hua Later, serious internal root decay was observed, and only residual fibrous vascular bundles with a brown or reddish-brown color remained (Fig. 1A, D). The aboveground leaves gradually turned yellow from the outside toward the inside; ultimately leading to the death of the entire plant.

3.2. Pathogenicity test of the strain isolated on P. cyrtonema Hua

Twenty-two strains were isolated from the rhizomes of *P. cyrtonema* Hua. The conidia were inoculated in the rhizomes of healthy *P. cyrtonema* Hua plants. After 7 days of inoculation with the ZW0619 strain, the rhizome's color began to change, and after 10 days, brown spots appeared on the surface of the rhizomes.. After 14 days, the surface of the rhizomes began to rot with white mycelium, and the symptoms observed were consistent with those in the field, indicating strong pathogenicity. Moreover, because of the later lesions on the roots, the rotten parts appeared concave, which is similar to root rot (Fig. 1B, E). While the plants inoculated with sterile water showed no symptoms (Fig. 1C, F). According to Koch's postulate, the pathogens were

sampled again after inoculation, separated and purified. All isolated strains were the same as the original inoculated strain, confirming that strain ZW0619 was the causal pathogen of root rot in *P. cyrtonema* Hua.

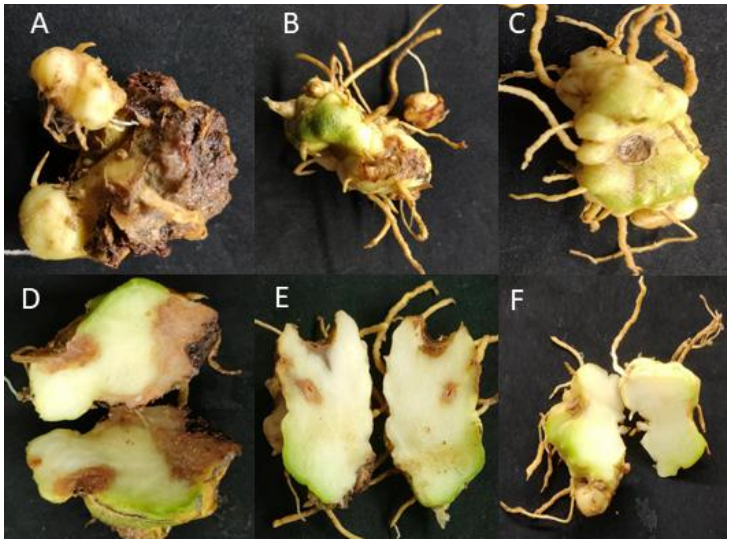

Figure 1. Field symptoms and pathogenicity verification. **(A, D)** Natural field symptoms of root rot in *P. cyrtonema* Hua. **(B, E)** Symptoms 2 weeks after artificial inoculation of the isolate ZW0619. **(C, F)** Symptoms 2 weeks after artificial inoculation with sterile water.

3.3. Morphological characterization

Once the virulence of strain ZW0619 was determined, morphological analyses of its colonies and spores were conducted. The colonies were initially milky white and fluffy, which gradually turned pale yellow or pinkish purple, and had a red halo with an off-white edge on the reverse side of the PDA plate. There was less hypha in the middle of the plate, while the edge hypha was developed (Fig. 2A). The macroconidia, as observed in the fungi culture on CLA, had 2-4 septa and were slender, sickle-shaped, or almost straight, with an average size of approximately 24.2-59.7 x 3.6-7.5 μm (n=50) (Fig. 2B). The chlamydospores were round and measured 11.8 ± 1.9 μm in size. (Fig. 2D, E).

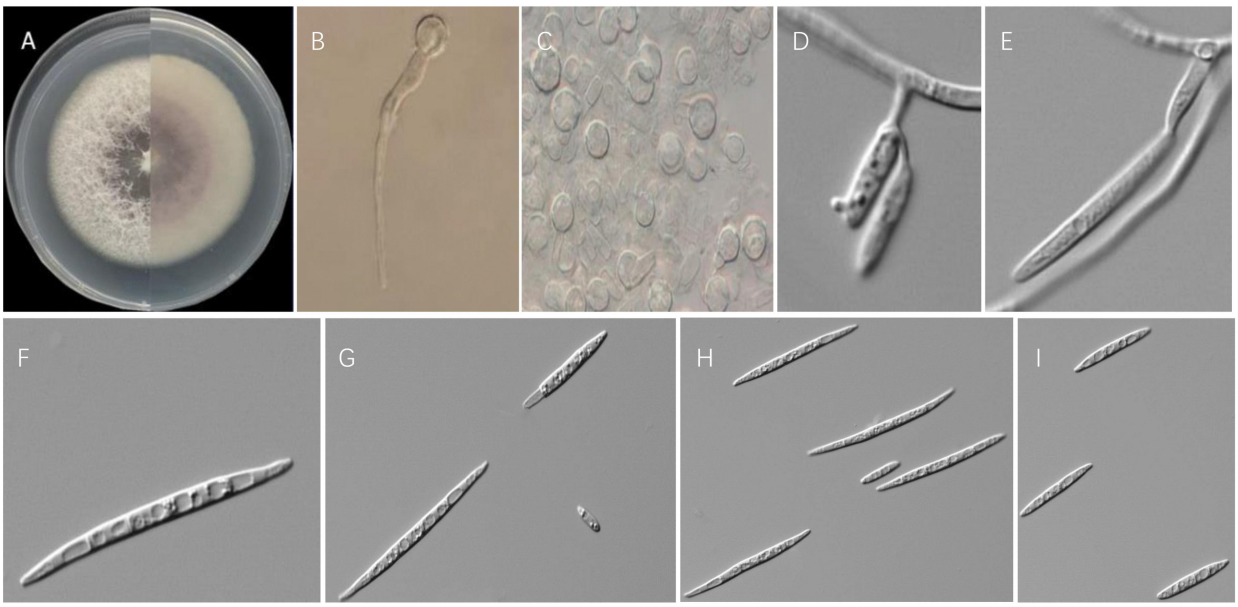

Figure 2. (A) Colony morphology of strain ZW0619 on potato dextrose agar (PDA), **(B, C)** chlamydospore of strain ZW0619, **(D, E)** macroconidia of strain ZW0619 on septate mycelium, **(F–I)** macroconidia of strain ZW0619. Scale bars: B, C = 10 μm; D–I = 50 μm.

3.4. Molecular identification of the pathogen

In this study, the *RPB2*, *EF-1α*, and *TUB2* fragments of the pathogenic fungus were amplified using the isolated and purified mycelium as material and genomic DNA as the template. The PCR products were then recovered and sequenced. Sequence alignments of RNA polymerase II encoding the second largest subunit (*RPB2*), the translation elongation factor 1 alpha (*EF-1α*), and beta-tubulin (*TUB2*) from ZW0619 and a reference strain (obtained from GenBank) were generated (Table 3). A phylogenetic tree was constructed based on *RPB2-EF-1α-TUB2* (Maryani et al. 2019). Using *Fusarium acutatum* NRRL 54218 as the outgroup, the strain ZW0619 (GenBank accessions: *TEF-1α*, OP204202; *RPB2*, OP204203; *TUB2*, OP292972) and *F. commune* were clustered into a single group with a bootstrap support value of 98% (Fig. 3), which is consistent with morphological and molecular identification results.

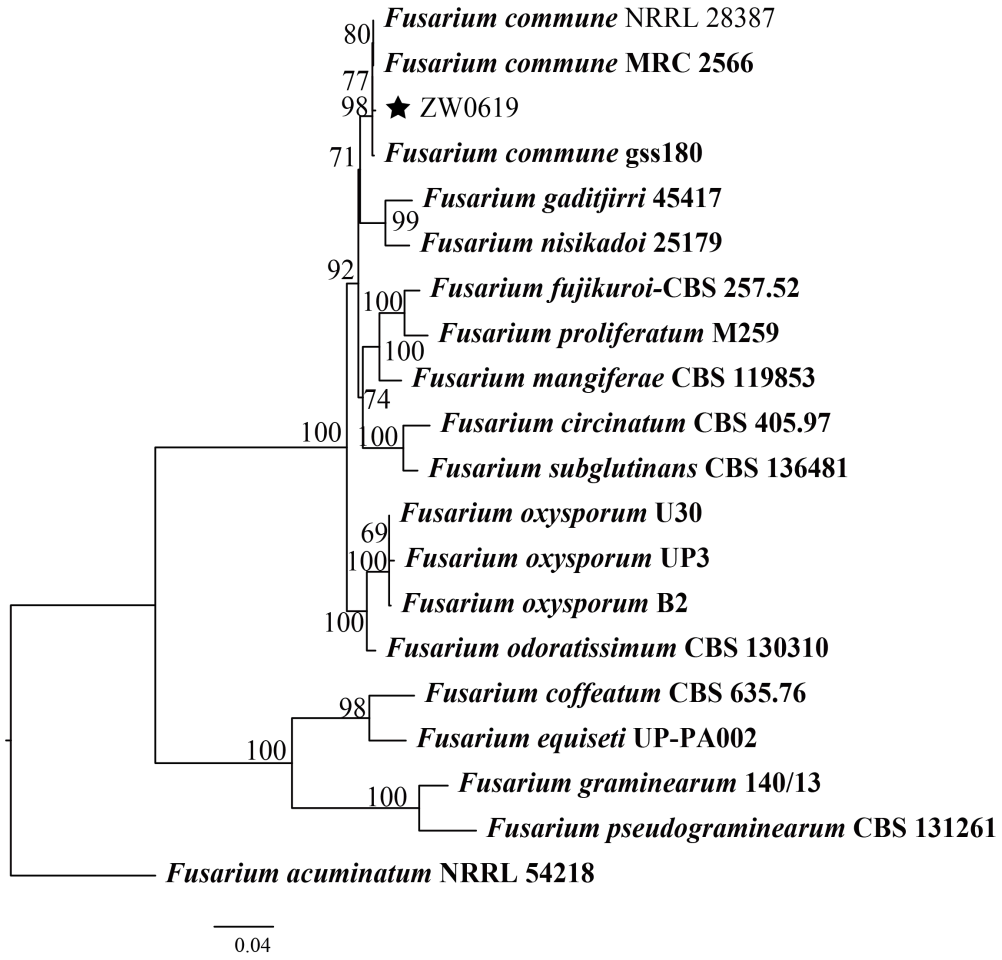

Figure 3. Best scoring RAxML tree obtained from the combined sequence alignment of *rpb2, tef1-α*, and β-tubulin of *Fusarium* spp. Bootstrap support values and maximum parsimony posterior probabilities are given at each node based on 1000 bootstrap replicates. *Fusarium acutatum* NRRL 54218 was used as the outgroup. The five-pointed star indicates the new isolate in this study.

Table 3. Reference isolates used in this study and GenBank accession numbers.

Species	Culture Collection Accession Numbers	GenBank Accession		
		TEF-1α	RPB2	TUB
Fusarium commune	ZW0619	OP204202	OP204203	OP292972
Fusarium fujikuroi	CBS 257.52	MW402119	MW402812	KU603885

Fusarium oxysporum	B2	MN754062	-	MN754078
Fusarium proliferatum	M259	KJ555080	-	KJ544176
Fusarium graminearum	140/13	KP400720	-	KP710664
Fusarium coffeatum	CBS 635.76	MN120755	MN120736	-
Fusarium subglutinans	CBS 136481	KU711692	KU604282	KU603893
Fusarium mangiferae	CBS 119853	MN534016	MN534270	MN534140
Fusarium pseudograminearum	CBS 131261	JQ429338	JX162517	-
Fusarium odoratissimum	CBS 130310	MH485013	MH485013	MH485104
Fusarium equiseti	UP-PA002	MH521297	-	MH521296
Fusarium circinatum	CBS 405.97	KM231943	MN534252	KM232080
Fusarium oxysporum	UP3	MN754063	-	MN754079
Fusarium oxysporum	U30	MN754061	-	MN754077
Fusarium commune	gss180	MH341219	-	MH341249
Fusarium commune	NRRL 28387	AF246832	JX171638	JX171638
Fusarium commune	MRC 2566	MH582348	MH582181	-
Fusarium gaditjirri	45417	MN193881	MN193909	-
Fusarium nisikadoi	25179	MN193879	MN193907	-
Fusarium acuminatum	NRRL 54218	HM068316	HM068336	-

3.5. Biological characteristics of ZW0619

After being cultured for 5 days under different temperatures, ZW0619 showed a colony diameter of 19.83 mm at 10℃, 28 mm at 15℃, 45.67 mm at 20℃, 73.67 mm at 25℃, 66.17 mm at 28℃, and 59.33 mm at 30℃ (Fig. 4A). These results demonstrate that 25℃ was the most suitable temperature for the growth of ZW0619.. The isolate was able to grow in pH conditions ranging from 4 to 11, reaching a maximum colony diameter of 61.33 mm at pH 8, indicating that this was the most optimum pH for growth (Fig. 4B). ZW0619 was able to grow on all the tested carbon and nitrogen sources. However, it showed the fastest growth on soluble starch and peptone compared to other carbon and nitrogen sources. Soluble starch was the optimal carbon source while peptone was the optimal nitrogen source for its growth (Fig. 4C). When exposed to 24 hours of full light, the mycelia of ZW0619 showed the most favorable growth (Fig. 5). In summary, the results showed that ZW0619 can grow in a wide range of pH and temperature conditions. The strain prefers soluble starch and peptone as carbon and nitrogen sources, and full light for growth. These findings provide useful information for the management and control of root rot caused by ZW0619 in *P. Cyrtonema* Hua.

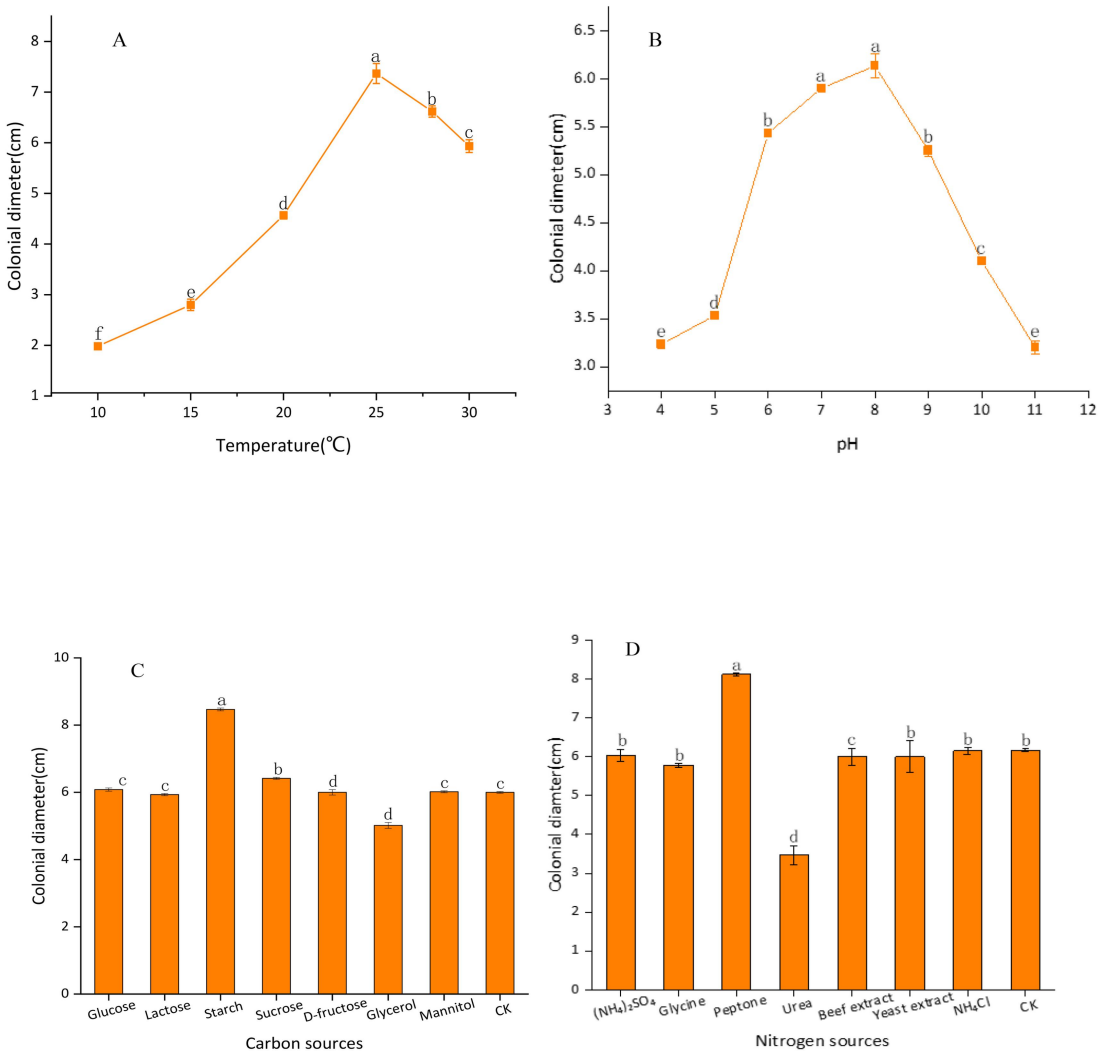

Figure 4. Effects of temperature, pH, carbon, and nitrogen sources on mycelial growth of F. commune ZW0619. **(A)** Colony diameter under different temperatures. (B) Colony diameter under different pH values. **(C)** Colony diameter under different carbon sources. **(D)** Colony diameter under different nitrogen sources. Different lowercase letters indicate significant differences ($P < 0.05$). Data are presented as mean ± S.D. ($n = 3$).

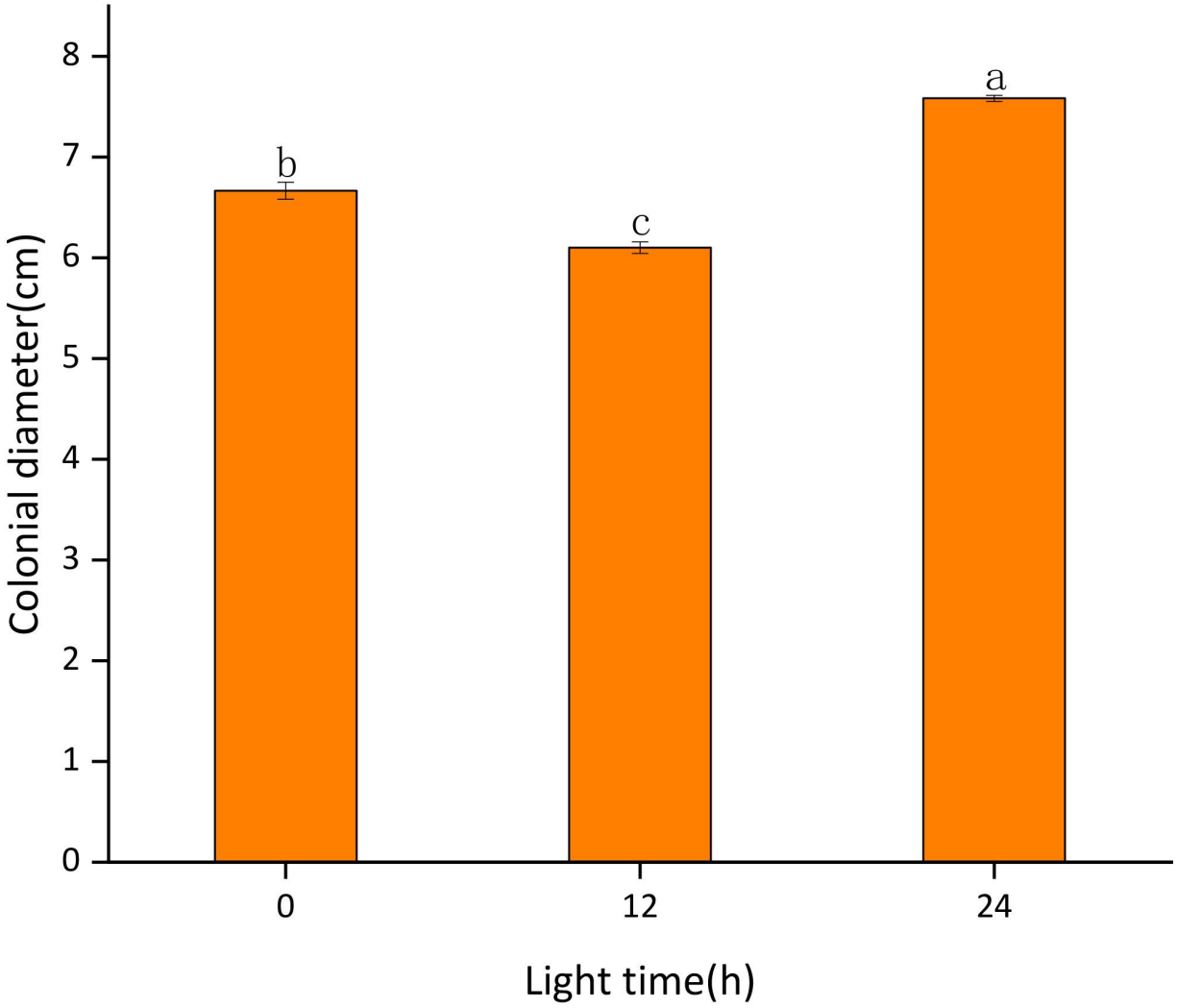

253

254 **Figure 5.** Effects of photoperiod on mycelial growth of *F. commune* ZW0619. Different lowercase letters indicate significant differences (P <
255 0.05). Data are presented as means ± S.D. (n = 3).

256 **3.6. Toxicity of** phytochemicals **against F. commune ZW0619**

257 Figure 6 and Table 4 present the inhibitory activity of seven phytochemicals (2-allylphenol, eugenol, carvacrol, geraniol,
258 cinnamaldehyde, magnolol, and honokiol) on the mycelial growth of *F. commune* ZW0619. . Regression analyses showed a
259 positive correlation between concentration and pathogen growth inhibition with R^2 values close to 1,indicating that all equations
260 were reliable.. The results showed that the phytochemicals had different levels of inhibitory effects on the pathogen. Honokiol >
261 magnolol > 2-allylphenol > carvacrol > eugenol > cinnamaldehyde > geraniol exhibited decreasing antifungal activities..
262 Honokiol, magnolol, 2-allylphenol, and carvacrol showed a clear inhibitory effect on *F. commune* with EC_{50} values below 100
263 mg/L. The EC_{50} value for Honokiol was 8.2628 ± 0.27 mg/L. Eugenol and cinnamaldehyde also exhibited a certain inhibitory
264 effect,, with the EC_{50} values of 107.5953 ± 0.19 and 150.5492 ± 0.14 mg/L, respectively. The antifungal effect of geraniol was

265 relatively weak with an EC_{50} value of 260.7979 ± 0.18 mg/L. Therefore, honokiol exhibated the potential to control root rot in *P.*

266 *cyrtonema* Hua.

267 In conclusion, the results provide valuable information on the inhibitory effects of different phytochemicals on the root rot
268 pathogen in P. Cyrtonema Hua. The findings demonstrate that honokiol, magnolol, 2-allylphenol, and carvacrol can be used to
269 control root rot, with honokiol exhibiting the highest antifungal activity. These results offer important insights into the
270 development of natural and environmentally friendly treatments for root rot disease in crops.

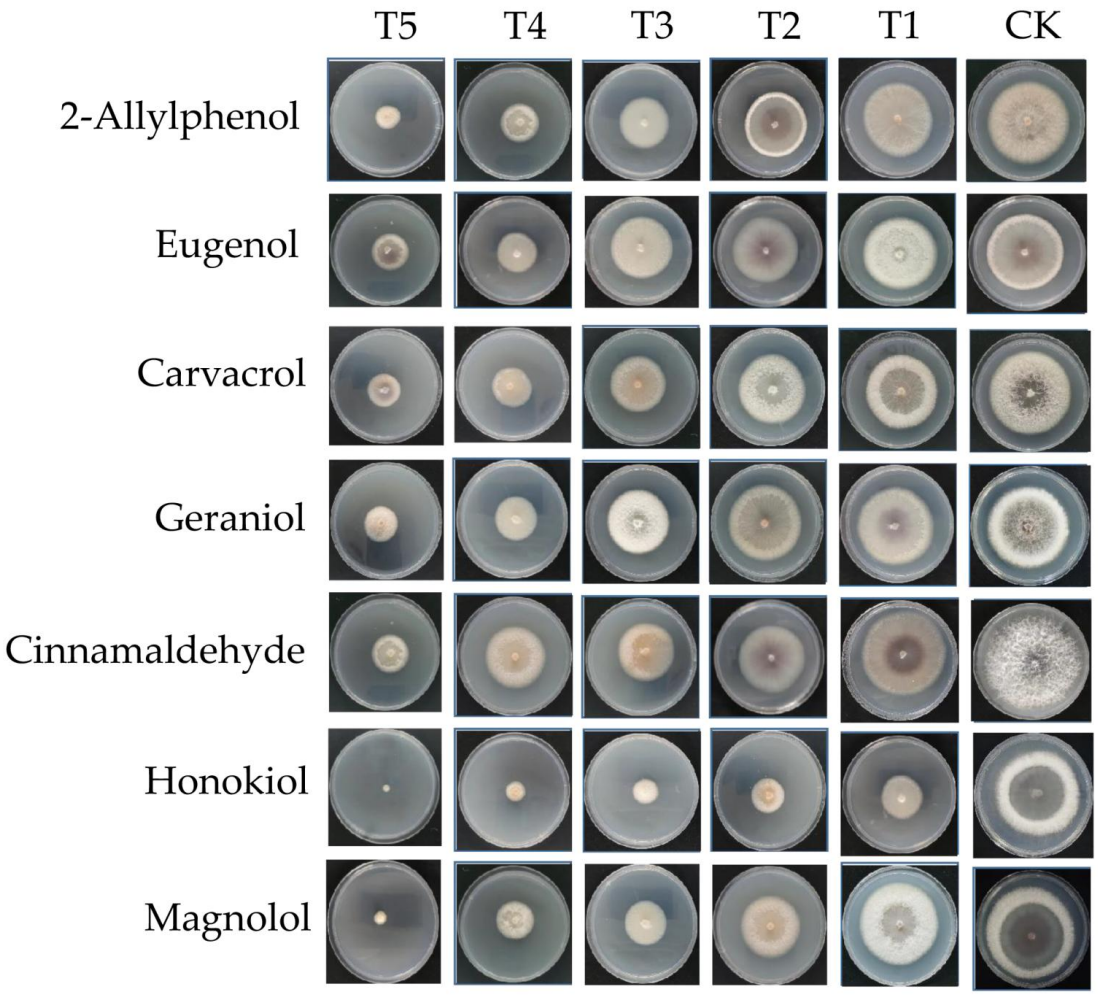

271

272 **Figure 6.** Mycelial growth inhibition of *Fusarium commune* ZW0619 after the application of different phytochemicals at various concentrations,
273 with fungicide-free plates (C.K.) as the control.

274 **Table 4.** Toxicities of different phytochemicals against *Fusarium commune*.

Active Ingredients of Biological Fungicides	Regression Equation	EC_{50} (μg mL^{-1})	r	95% Confidence Inte
2-Allylphenol	y=0.0463+2.8861x	52.0474±0.12	0.9588	38.3701–70.6000
Eugenol	y=0.7333+2.1000x	107.5953±0.19	0.9861	74.6016–155.181
Carvacrol	y=0.3541+2.6311x	58.3143±0.44	0.9464	41.5224–81.8969
Geraniol	y=3.5617+0.5953x	260.7979±0.18	0.9524	61.2590–1110.295
Cinnamaldehyde	y=0.0084+2.2922x	150.5492±0.14	0.9835	100.3333–225.897
Honokiol	y=4.0944+0.9874x	8.2628±0.27	0.9727	2.2854–29.8734
Magnolol	y=1.5534+2.0305x	49.8209±0.23	0.9667	34.7621–71.4030

Each value indicates the mean ± S.D. of three replicates; X and Y represent the phytochemical concentrations and growth inhibition rate for active ingredients, respectively.

4. Discussion

Polygonatum (Huangjing in Chinese) is a wildly used multi-purpose material in food and medicine (Hu et al. 2022). However, severe root rot has been reported, in recent years, causing rhizome rot and plant death in severe cases, leading to a significant impact. on the quality and yield of the plant. The root rot is caused by various soil-borne pathogens,. One of the most important pathogens is *Fusarium*(division Ascomycota), which has a wide range of hosts, including corn, soybean, and wheat crops, as well as horseradish (Yu and Babadoost 2013). Furthermore, *Fusarium* sp. has wide geographic and host ranges (Al-Sadi et al. 2014; Rahman and Punja 2005; Stefańczyk et al. 2016; Parikh 2018). To the best of our knowledge, this is the first report of *F. commune* causing root rot in *P. Cyrtonema* Hua. These findings provide important insights for the management and control of root rot in *P. Cyrtonema* Hua and other susceptible crops.

F. commune has various modes of transmission, including through chlamydospores and macroconidia that can be carried by air, rain, and insects (Husna 2020; Yang et al. 2022; Heck 2018; Chen et al. 2021; Shimwela et al. 2016). Additionally, environmental and nutritional factors, such as temperature, pH, carbon and nitrogen sources, and light, can significantly affect the pathogen infection (Moreno-Amores et al. 2020; Alves et al. 2017; Liu et al. 2017; Anja et al. 2021). However, knowledge of the biological characteristics of *F. commune* is limited. Previous studies have s reported that the optimal growth temperature for related pathogens, such as *Fusarium meridionale*, *Fusarium poae*, and *Fusarium graminearum*, is 25℃ (Rybecky et al. 2018; Nazari et al. 2018; Chen et al. 2022b). Our results are in consistent with those findings. Moreover, Zhao et al. (2019) reported that *F. graminearum* grows best in a neutral or alkaline medium. Similarly, the current study found that mycelia grew fastest at pH 8. These findings can help to develop optimal environmental conditions for growth and control measures for *F. commune* in *P. Cyrtonema* Hua and crops susceptible to this pathogen..

The carbon source can also have an impact on the secondary metabolism of *Fusarium*. Achimón et al. (2019) demonstrated that carbon sources affect the secondary metabolism of *Fusarium verticillioides*, a pathogen that infects maize, whilth starch promoting fungal growth. In this study, mycelia grew in all the carbon sources tested, and the fastest growth was observed in the medium with soluble starch as a carbon source. Similar to our findings, *Fusarium avenaceum* and *F. graminearum* were reported to grow fastest in medium with soluble starch as a carbon source (Tang et al. 2022; Chen et al. 2022b). The types of carbohydrates used as an energy source may influence the production, liberation, and germination of zoospores outside the root and oospore formation inside the root (Papavizas and Ayers 1964). Further research is required to determine how various carbon sources affect pathogen growth. These findings could provide insight into the management and control of root rot in *P. Cyrtonema* Hua and other crops affected by *F. commune.*

The effect of nitrogen on plant resistance to pathogens can vary, as increasing nitrogen has been reported to either increase or decrease plant resistance depending on the pathogen's infection strategy (Mur et al. 2017). Typically, during infection, pathogens use available nutrient sources for growth while evading or tolerating host defenses (Boyce et al. 2015). In our study, we observed that *F. commune* grew fastest in peptone and slowest in urea. Therefore, urea can be used as a nitrogen fertilizer for *P. Cyrtonema* Hua plants, providing nutrients to the plant and potentially slowing down the growth of *F. commune*. These findings could contribute to the development of integrated pest management strategies that include optimizing nitrogen sources to promote plant growth while limiting the negative impact of *F. commune* on plant health.

Photoperiod is a critical environmental factor that can influencethe growth and pathogenesis of plant pathogens (Rasiukevičiūtė et al. 2021; Costa et al. 2021; Macioszek et al. 2021). In our study, we observed that full light was beneficial for

the growth of the *F. commune* ZW0619 mycelia. Studies have shown that that *F. oxysporum* hyphae can grow under alternating light and dark periods (Shao et al. 2014). Tang et al. (2022) found that an alternating cycle of 8 h of light and 16 h of dark is beneficial for the growth of *F. avenaceum* hyphae. However, Costa et al. (2020) did not observe a significant difference in the germination and growth of *F. fujikuroi* under different light and dark conditions. Hence, the response of mycelial growth to photoperiod could be widespread among *Fusarium* spp. These findings suggest the importance of considering photoperiod as a factor in the development of management strategies for Fusarium related plant diseases. Chemical fungicides are commonly used as the main control measure for plant pathogens (Tang et al. 2022; Chen et al. 2022c). However, their improper use can pose safety hazards. Long-term use of chemical fungicides can also lead to pathogen resistance, further complicating disease management (Romanazzi et al. 2016; Chaves et al. 2022; Choi et al. 2017). In recent years, there has been increasing attention to the potential health risks associated with synthesized fungicides, (Valcke et al. 2017; Gonçalves et al. 2021; García-Machado et al. 2022). As an alternative to synthetic fungicides, biological agents, such as phytochemicals, have emerged as a sustainable and environmentally friendly option that complies with integrated pest management and organic farming regulations (Zhang et al. 2020; Lamichhane et al. 2016). Therefore, the expanded use of phytochemicals to control pathogens is an important goal. In this study, inhibitory effects of seven phytochemicals against *F. commune* ZW0619 based on mycelial growth rate were studied. with four phytochemicals found to have notable antifungal effects, and honokiol demonstrating the strongest in-hibition (EC_{50} = 8.2628 ± 0.27 mg/L). Essential oils are aromatic substances extracted from plants, with terpenes and their oxides, as well as sesquiterpenes, being the main components. Moreover, aldehydes, alcohols, and phenolic compounds have shown certain antifungal activities in previous studies (Xie et al. 2017; Lee et al. 2010). Phytochemicals have a low risk of resistance development and high antifungal activity, and are considered safe and environmentally friendly..Honokiol has been found to inhibit other fungi, such as *Alternaria alternata* and *Rhizoctonia solani* (Chen et al. 2019; Yan et al. 2020; Wang et al. 2022). However, as this was a laboratory experiment, further research is needed to verify the field control effect of these phytochemicals against plant pathogens. Additionally, the antifungal mechanisms of these phytochemicals require further investigation.

5. Conclusion

In this study, the causative agent of *P. cyrtonema* Hua root rot was identified as *F. commune* based on morphological identification, molecular biological characteristics, and pathogenicity tests. This is the first report of *F. commune* as a causative agent for root rot of *P. cyrtonema* Hua. The biological characteristics of *F. commune* ZW0619 were studied, and the inhibitory effects of seven phytochemicals on the growth of *F. commune* ZW0619 were evaluated. These findings enhance our understanding of the factors contributing to *P. cyrtonema* Hua root rot and hold significant implications for the prevention and control of this diease.

Acknowledgements

This research is supported by the National Key Research and Development Program (No. 2021YFD1601002-03). We thank Guangming Wang for assisting with disease investigation and sampling.

References

Achimón F, Dambolena J S, Zygadlo J A, Pizzolitto R P (2019) Carbon sources as factors affecting the secondary metabolism of the maize pathogen *Fusarium verticillioides*. LWT 115:108470

349 Al-Sadi A M, Al-Ghaithi A G, Al-Fahdi N, Al-Yahyai R (2014) Characterization and Pathogenicity of Fungal Pathogens
350 Associated with Root Diseases of Citrus in Oman. Int J Agric Biol 16:371-376.
351 Alves R, Mota S, Silva S, Rodrigues C F, Brown A J, Henriques M, Casal M, Paiva S (2017) The carboxylic acid transporters
352 Jen1 and Jen2 affect the architecture and fluconazole susceptibility of Candida albicans biofilm in the presence of lactate.
353 Biofouling 33:943-954.
354 Alzahrani A, Ouahmane L, Aboul-Soud M A M, Giesy J P, Bouia A (2022) Lavandula dentata L.: Phytochemical Analysis,
355 Antioxidant, Antifungal and Insecticidal Activities of Its Essential Oil. Plants 11:311.
356 Anja D J, Marjolein K H, Weerheim K, Leiss K (2021) LED Lighting Strategies Affect Physiology and Resilience to Pathogens
357 and Pests in Eggplant (*Solanum melongena* L.). FRONT PLANT SCI 11:610046.
358 Arunachalam C, Doohan F M (2013) Trichothecene toxicity in eukaryotes: cellular and molecular mechanisms in plants and
359 animals. TOXICOL LETT 217:149-158.
360 Audenaert K, Vanheule A, Höfte M, Haesaert G (2013) Deoxynivalenol: a major player in the multifaceted response of Fusarium
361 to its environment. Toxins 6:1-19.
362 Barbett K, Wong D H, Sivasithamparam (1987) Fungicidal seed treatments for control of root rot in subterranean clover.
363 Phytophylactica Plant Protection Sciences & Microbiology 19.
364 Boyce K J, McLauchlan A, Schreider L, Andrianopoulos A (2015) Intracellular growth is dependent on tyrosine catabolism in the
365 dimorphic fungal pathogen *Penicillium marneffei*. PLoS Pathog 11:e1004790.
366 Chaves M A, Reginatto P, Costa B S, Paschoal R I, Teixeira M L, Fuentefria A M (2022) Fungicide Resistance in *Fusarium*
367 *graminearum* Species Complex. CURR MICROBIOL 79:62.
368 Chen J, Ran F, Shi J, Chen T, Zhao Z, Zhang Z, He L, Li W, Wang B, Chen X, Wang W, Long Y (2022b) Identification of the
369 Causal Agent of Brown Leaf Spot on Kiwifruit and Its Sensitivity to Different Active Ingredients of Biological Fungicides.
370 Pathogens 11:673.
371 Chen S C, Yang C S, Chen J J (2022a) Main Bioactive Components and Their Biological Activities from Natural and Processed
372 Rhizomes of *Polygonum sibiricum*. Antioxidants (Basel) 11:1383.
373 Chen T, Wu X, Dai Y, Yin X, Zhao Z, Zhang Z, Li W, He L, Long Y (2022c) Sensitivity Testing of Natural Antifungal Agents on
374 *Fusarium fujikuroi* to Investigate the Potential for Sustainable Control of Kiwifruit Leaf Spot Disease. J. Fungi 8: 239.
375 Chen Y, Zhu X, Hou Z, Wang Y, Zhou Y, Wang L, Liu L, Duan J, Jibril S M, Li C (2021) RNA-Based Analysis Reveals High
376 Diversity of Plant-Associated Active Fungi in the Atmosphere. FRONT MICROBIOL 12:683266.

377 Chen Y H, Lu M H, Guo D S, Zhai Y Y, Miao D, Yue J Y, Yuan C H, Zhao M M, An D R (2019) Antifungal Effect of Magnolol
378 and Honokiol from Magnolia officinalis on *Alternaria alternata* Causing Tobacco Brown Spot. Molecules 24:2140.
379 Choi H W, Hong S K, Lee Y K, Kim W G (2014) First Report of *Fusarium succisae* Causing Flower Rot on Thread-leaf
380 Coreopsis. Plant Dis 98:1002.
381 Choi I Y, Choi J N, Sharma P K, Lee W. H (2010) Isolation and Identification of Mushroom Pathogens from Agrocybe aegerita.
382 Mycobiology 38:310-315.
383 Choi Y, Jung B, Li T, Lee J (2017) Identification of Genes Related to Fungicide Resistance in *Fusarium fujikuroi*. Mycobiology
384 45:101-104
385 Costa T P, Rodrigues E M, Dias L P, Pupin B, Ferreira P C, Rangel D E. (2021) Different wavelengths of visible light influence
386 the conidial production and tolerance to ultra-violet radiation of the plant pathogens *Colletotrichum acutatum* and *Fusarium*
387 *fujikuroi*. Eur. J. Plant Pathol 159:105-115
388 Deng S, Ma X, Chen Y, Feng H, Zhou D, Wang X, Zhang Y, Zhao M, Zhang J, Daly P, Wei L. (2022) LAMP Assay for
389 Distinguishing *Fusarium oxysporum* and *Fusarium commune* in Lotus (*Nelumbo nucifera*) Rhizomes. Plant Dis 106:231-246
390 Detranaltes C, Saldanha M, Scofield S R, Cai G (2022) First report of *Fusarium commune* causing root rot of soybean seedlings in
391 Indiana. Plant Dis.
392 El Abdali Y, Agour A, Allali A, Bourhia M, El Moussaoui A, Eloutassi N, Salamatullah A M, Alzahrani A, Ouahmane L,
393 Aboul-Soud M A M, Giesy J P, Bouia A (2022) Lavandula dentata L.: Phytochemical Analysis, Antioxidant, Antifungal and
394 Insecticidal Activities of Its Essential Oil. Plants (Basel) 11:311
395 Elshafie H S, Caputo L, Martino L, Gruľová D, Zheljazkov V Z, Feo V, Camele I (2010) Biological investigations of essential oils
396 extracted from three Juniperus species and evaluation of their antimicrobial, antioxidant and cytotoxic activities. J APPL
397 MICROBIOL 129:1261-1271.
398 García-Machado F J, García-García A L, Borges A A, Jiménez-Arias D (2022) Root treatment with a vitamin K3 derivative: a
399 promising alternative to synthetic fungicides against *Botrytis cinerea* in tomato plants. PEST MANAG SCI 78: 974-981.
400 Glass N L, Donaldson G C (1995) Development of primer sets designed for use with the PCR to amplify conserved genes from
401 filamentous ascomycetes. APPL ENVIRON MICROB 61:1323-1330
402 Gonçalves D D C, Ribeiro W R, Gonçalves D C, Menini L, Costa H (2021) Recent advances and future perspective of essential
403 oils in control Colletotrichum spp.: A sustainable alternative in postharvest treatment of fruits. Food Res. Int 150:110758
404 Heck M (2018) Insect Transmission of Plant Pathogens: a Systems Biology Perspective. mSystems 3:e00168-17

405 Hu Y, Yin M, Bai Y, Chu S, Zhang L, Yang M, Zheng X, Yang Z, Liu J, Li L, Huang L, Peng H (2022) An Evaluation of Traits,
406 Nutritional, and Medicinal Component Quality of *Polygonatum cyrtonema Hua* and *P. sibiricum* Red. FRONT PLANT SCI
407 13:891775
408 Husna A (2020) *Fusarium commune* associated with wilt and root rot disease in rice. Plant Pathol 69
409 Kaur S, Barakat R, Kaur J, Epstein L (2022) The Effect of Temperature on Disease Severity and Growth of *Fusarium oxysporum* f.
410 sp. apii Races 2 and 4 in Celery. Phytopathology 112:364-372
411 Khan H, Saeed M, Gilani A U, Khan M A, Dar A, Khan I (2010) The antinociceptive activity of Polygonatum verticillatum
412 rhizomes in pain models. J Ethnopharmacol 127:521-527
413 Kim C, Bushlaibi M, Alrefaei R, Ndegwa E, Kaseloo P, Wynn C (2019) Influence of prior pH and thermal stresses on thermal
414 tolerance of foodborne pathogens. Food Sci. Nutr 7:2033-2042
415 Kim S, Lee D G (2018) Isoquercitrin, a phytochemical derived from Aster yomena, improves convetional antibiotics affect
416 through reactive oxygen species accumulation in Candida albicans. FREE RADICAL BIO MED 128:S79-S97
417 Kimura M (1980) A simple method for estimating evolutionary rates of base substitutions through comparative studies of
418 nucleotide sequences. J MOL EVOL 16:111-120
419 Kumar S, Stecher G, Li M, Knyaz C, Tamura K (2018) MEGA X: Molecular Evolutionary Genetics Analysis across Computing
420 Platforms. Mol. Biol. Evol 35:1547-1549
421 Lamichhane J R, Dachbrodt-Saaydeh S, Kudsk P, Messéan A (2016) Toward a Reduced Reliance on Conventional Pesticides in
422 European Agriculture. Plant Dis 100:10-24
423 Lee Y S, Kim J, Shin S C, Lee S G, Park I k (2010) Antifungal activity of Myrtaceae essential oils and their components against
424 three phytopathogenic fungi. FLAVOUR FRAG J 23:23-28
425 Lima A, Ala L, Sousa J P, Pinheiro L S, Oliveirafilho A A, P J, Lima E O (2017) Antifungal Activity of Geraniol on Candida
426 albicans Isolates of Pediatric Clinical Importance. Int. J. Pharmacogn.
427 Liu J, Sui Y, Wisniewski M, Xie Z, Liu Y, You Y, Zhang X, Sun Z, Li W, Li Y, Wang Q (2017) The impact of the postharvest
428 environment on the viability and virulence of decay fungi. Crit Rev Food Sci Nutr 58:1681-1687
429 Liu S, Jia Q J, Peng Y Q, Feng T H, Hu S T, Dong J E, Liang Z S (2022) Advances in Mechanism Research on Polygonatum in
430 Prevention and Treatment of Diabetes. FRONT PHARMACOL 13:758501
431 Lookabaugh E C, Kerns J P, Shew B B (2021) Evaluating Fungicide Selections to Manage Pythium Root Rot on Poinsettia
432 Cultivars with Varying Levels of Partial Resistance. Plant Dis 105:1640-1647

433 Luo S, Zhang X, Huang S, Feng X, Zhang X, Xiang D (2022) A monomeric polysaccharide from *Polygonatum sibiricum*
434 improves cognitive functions in a model of Alzheimer's disease by reshaping the gut microbiota. Int. J. Biol. Macromol
435 213:404-415
436 Macioszek V K, Sobczak M, Skoczowski A, Oliwa J, Michlewska S, Gapińska M, Ciereszko I, Kononowicz A K (2021) The
437 Effect of Photoperiod on Necrosis Development, Photosynthetic Efficiency and 'Green Islands' Formation in Brassica juncea
438 Infected with *Alternaria brassicicola.* INT J MOL SCI 22:8435
439 Maresca M (2013) From the gut to the brain: journey and pathophysiological effects of the food-associated trichothecene
440 mycotoxin deoxynivalenol. Toxins 5:784-820
441 Maryani N, Sandoval-Denis M, Lombard L, Crous P W, Kema G H J (2019) New endemic Fusarium species hitch-hiking with
442 pathogenic Fusarium strains causing Panama disease in small-holder banana plots in Indonesia. Persoonia 43:48-69
443 Mezzalama M, Guarnaccia V, Martino I, Tabome G, Gullino M L (2021) First report of *Fusarium commune* causing root and
444 crown rot on maize in Italy. Plant Disease.
445 Mo F, Hu X, Ding Y, Li R, Long Y, Wu X, Li M (2021) Naturally produced magnolol can significantly damage the plasma
446 membrane of *Rhizoctonia solani*. Pestic Biochem Physiol 178:104942
447 Moreno-Amores J, Michel S, Lschenberger F, Buerstmayr H (2020) Dissecting the Contribution of Environmental Influences,
448 Plant Phenology, and Disease Resistance to Improving Genomic Predictions for Fusarium Head Blight Resistance in Wheat.
449 Agronomy 10:2008
450 Mottaghipisheh J, Stuppner H (2021) A Comprehensive Review on Chemotaxonomic and Phytochemical Aspects of
451 Homoisoflavonoids, as Rare Flavonoid Derivatives. INT J MOL SCI 22:2735
452 Mur L A, Simpson C, Kumari A, Gupta A K, Gupta K J (2017) Moving nitrogen to the centre of plant defence against pathogens.
453 *Ann. Bot* 119:703-709
454 Nazari L, Pattori E, Manstretta V, Terzi V, Morcia C, Somma S, Moretti A, Ritieni A, Rossi V (2018) Effect of temperature on
455 growth, wheat head infection, and nivalenol production by *Fusarium poae*. Food Microbiol 76:83-90
456 Nosratabadi M, Kachuei R, Rezaie S, Harchegani A B (2018) Beta-tubulin gene in the differentiation of Fusarium species by
457 PCR-RFLP analysis. Le infezioni in medicina 26:52-60
458 O'Donnell K, Kistler H C, Cigelnik E, Ploetz R C (1998) Multiple evolutionary origins of the fungus causing Panama disease of
459 banana: concordant evidence from nuclear and mitochondrial gene genealogies. Proc. Natl. Acad. Sci.U.S.A 95:2044-2049

O'Donnell K, Sutton D A, Rinaldi M G, Sarver B A, Balajee S A, Schroers H J, Summerbell R C, Robert V A, Crous P W, Zhang N, Aoki T, Jung K, Park J, Lee Y H, Kang S, Park B, Geiser D M. 2010. Internet-accessible DNA sequence database for identifying fusaria from human and animal infections. J CLIN MICROBIOL 48:3708-3718

Osawa H, Yu S, Akino S, Kondo N (2020) Autumn potato seedling failure due to potato dry rot in Nagasaki Prefecture, Japan, caused by *Fusarium acuminatum* and *Fusarium commune*. J GEN PLANT PATHOL pp:1-5

Özer G, Paulitz T C, Imren M, Alkan M, Muminjanov H, Dababat A A (2020) Identity and Pathogenicity of Fungi Associated with Crown and Root Rot of Dryland Winter Wheat in Azerbaijan. Plant Dis 104:2149-2157

Papavizas G C, Ayers W A. (1964) Effect of Various Carbon Sources on Growth and Sexual Reproduction of Aphanomyces Euteiches. Mycologia 56:816-830

Parikh L, Kodati S, Eskelson M J, Adesemoye A O. (2018) Identification and pathogenicity of Fusarium spp. In row crops in Nebraska. *Crop Prot* 108:120-127

Pinho F V, Cruz L C, Rodrigues N R, Waczuk E P, Souza C E, Coutinho H D, Costa J G, Athayde M L, Boligon A A, Franco J L, Posser T, Menezes I R (2016) Phytochemical Composition, Antifungal and Antioxidant Activity of Duguetia furfuracea A. St.-Hill. OXID MED CELL LONGEV 2016:7821051

Qu T, Gao S, Li J, Hao J J, Ji P (2017) Synthesis and antifungal activity of 2-allylphenol derivatives against fungal plant pathogens. Pestic Biochem Physiol 135:47-51

Rahman M, Punja Z K (2005) Biochemistry of ginseng root tissues affected by rusty root symptoms. Plant Physiol. Biochem 43:1103-1114

Rasiukevičiūtė N, Brazaitytė A, Vaštakaitė-Kairienė V, Kupčinskienė A, Duchovskis P, Samuolienė G, Valiuškaitė A (2015) The Effect of Monochromatic LED Light Wavelengths and Photoperiods on *Botrytis cinerea*. J. Fungi 7:970

Romanazzi G, Smilanick J L, Feliziani E, Droby S (2016) Integrated management of postharvest gray mold on fruit crops. Postharvest Biol. Technol. 113:69-76

Rybecky A I, Chulze S N, Chiotta M L (2018) Effect of water activity and temperature on growth and trichothecene production by *Fusarium meridionale*. Int. J. Food Microbiol. 285:69-73

Shao Q S, Liu H B, Zhao X F, Hu R H, Li M Y (2014) Biological characteristics of *Fusarium oxysporum* and inhibitory effects of five fungicides. Zhongguo Zhong Yao Za Zhi 39:1386-1390

Sharma S, Joshi R, Kumar D (2021a) Metabolomics insights and bioprospection of *Polygonatum verticillatum*: An important dietary medicinal herb of alpine Himalaya. Food Res. Int.148:110619

488 Sharma S, Kumar S (2021b) Fast and accurate bootstrap confidence limits on genome-scale phylogenies using little bootstraps.
489 Nat Comput 1:573-577
490 Shimwela M M, Ploetz R C, Beed F D, Jones J B, Blackburn J K, Mkulila S I, van Bruggen A H. (2016) Banana xanthomonas
491 wilt continues to spread in Tanzania despite an intensive symptomatic plant removal campaign: an impending
492 socio-economic and ecological disaster. Food Secur 8:939-951
493 Stefańczyk E, Sobkowiak S, Brylińska M, Śliwka J (2016) Diversity of Fusarium spp. associated with dry rot of potato tubers in
494 Poland. Eur. J. Plant Pathol.145:871–884
495 Tang X, Yang J G, Zhuoma G, Guo X, Cao P, Yi B, Wang W, Ji D, Pasquali M, Baccelli I, Migheli Q, Chen X, Cernava T (2022)
496 Biological characterization and *in vitro* fungicide screenings of a new causal agent of wheat Fusarium head blight in Tibet,
497 China. Front. Microbiol. 13:941734
498 Tays C, Guarnieri M T, Sauvageau D, Stein L Y (2018) Combined Effects of Carbon and Nitrogen Source to Optimize Growth of
499 Proteobacterial Methanotrophs. Front. Microbiol. 9:2239
500 Telli O, Jimenez-Quiros C, Mcdowell J M, Tör M (2020) Effect of light and dark on the growth and development of downy
501 mildew pathogen Hyaloperonospora arabidopsidis. Plant Pathol. 69.
502 Valcke M, Bourgault, M H, Rochette L, Normandin L, Samuel O, Belleville D, Blanchet C, Phaneuf D (2017) Human health risk
503 assessment on the consumption of fruits and vegetables containing residual pesticides: A cancer and non-cancer risk/benefit
504 perspective. Environ Int 108:63-74
505 Wang H, Chang K F, Hwang S F, Turnbull G D, Howard R J, Blade S F, Callan N W (2005) Fusarium root rot of coneflower
506 seedlings and integrated control using Trichoderma and fungicides. Biocontrol 50:317-329
507 Wang W, Dabu X, He J, Yang H, Yang S, Chen J, Fan W, Zhang G, Cai J, Ai H, Hai M (2019) Polygonatone H, a new
508 homoisoflavanone with cytotoxicity from *Polygonatum Cyrtonema* Hua. Nat. Prod. Res. 33:1727-1733
509 Wang X, Han X, Wang S, Wang Y, Wang P, Zhao Z, Qin H, Jing C, Liang C (2022) Extraction of honokiol from Artemisia argyi
510 and in vitro and in vivo investigation of its antifungal activity. Nat. Prod. Res. 4:1-6
511 Windham G L, Williams W P, Mylroie J E, Reid C X, Womack E D (2018) A Histological Study of Aspergillus flavus
512 Colonization of Wound Inoculated Maize Kernels of Resistant and Susceptible Maize Hybrids in the Field. *Frontiers in*
513 Microbiology 9:799
514 Wu J, Yu X, Wang X, Tang L, Ali S (2019) Matrine Enhances the Pathogenicity of Beauveria brongniartii Against *Spodoptera*
515 *litura* (Lepidoptera: Noctuidae). Front. Microbiol. 10:1812

516 Xie Y J, Wang Z J, Huang Q Q, Zhang D Y (2017) Antifungal activity of several essential oils and major components against
517 wood-rot fungi. Ind Crops Prod 108:278-285
518 Xing K, Liu Y, Shen X, Zhu X, Li X, Miao X, Feng Z, Peng X, Qin S (2017) Effect of O-chitosan nanoparticles on the
519 development and membrane permeability of Verticillium dahliae. Carbohydr. Polym165:334-343
520 Yan Y F, Yang C J, Shang X F, Zhao Z M, Liu Y Q, Zhou R, Liu H, Wu T L, Zhao W B, Wang Y L, Hu G F, Qin F, He Y H, Li
521 H X, Du S S (2020) Bioassay-guided isolation of two antifungal compounds from Magnolia officinalis, and the mechanism
522 of action of honokiol. Pestic Biochem Physiol 170:104705
523 Yang B, Zhao Y, Lu Y, Tao M, Wang Y, Guo Z (2022) First report of Alfalfa root rot caused by *Fusarium commune* in China.
524 Plant Dis.
525 Yang R, Miao J, Shen Y, Cai N, Wan C, Zou L, Chen J (2021) Antifungal effect of Cinnamaldehyde, Eugenol and Carvacrol
526 nanoemulsion against *Penicillium digitatum* and application in postharvest preservation of Citrus fruit. LWT 141:110924
527 Ye Q, Wang R, Ruan M, Yao Z, Cheng Y, Wan H, Li Z, Yang Y, Zhou G. 2020. Genetic Diversity and Identification of Wilt and
528 Root Rot Pathogens of Tomato in China. Plant Dis. 104:1715-1724
529 Yu J M, Babadoost M (2013) Occurrence of *Fusarium commune* and *F. oxysporum* in Horseradish Roots. Plant Dis 97:453-460
530 Zambounis A, Sytar O, Valasiadis D, Zoe H. 2020. Effect of photosensitizers on growth and morphology of Phytophthora
531 citrophthora coupled with leaf bioassays in pear seedlings. Plant Prot. Sci. 56:74-82
532 Zhang H, Godana E A, Sui Y, Yang Q, Zhang X, Zhao L (2020) Biological control as an alternative to synthetic fungicides for the
533 management of grey and blue mould diseases of table grapes: a review. Crit. Rev. Microbiol. 46:450-462
534 Zhang Y, Chen C, Zhao J, Chen C, Lin J, Jayawardena R S, Xiang M, Manawasinghe I S, You C (2021) *Fusarium elaeidis*
535 Causes Stem and Root Rot on Alocasia longiloba in South China. Pathogens 10:1395
536 Zhao L, Liu R, Gao H, Han Y, Wu W, Chen H (2019) Identification and Biological Characterization of Dominant Spoilage Fungi
537 From Postharvest Water Bamboo Shoot. J Agric Sci 33:2354-2361
538 Zhong Q, Xiao Y S, He B, Cao Z H, Shou Z G, Zhong J, Zhu J Z (2020) First Report of *Fusarium commune* causing Stem Rot of
539 Tobacco (*Nicotiana tabacum*) in Hunan Province, China. Plant Dis.
540 Zhou L, Zhang Z, Wei M, Xie Y, He S, Shi H, Lin Z (2019) Evaluation of the antifungal activity of individual and combined
541 monoterpenes against Rhizopus stolonifer and Absidia coerulea. Environ. Sci. Pollut. Res.26:7804-7809
542 Zhu L H, Xu W, Huang L, Ye J R, Li D W (2022) Pathogenicity and Biological Characteristics of Septotinia populiperda Causing
543 Leaf Blotch of Willow. Plant Dis 106:1262-1270